Thermodynamics and Energy Coupling in the Bacteriorhodopsin Photocycle†

György Váró‡ and Janos K. Lanyi*
Department of Physiology and Biophysics, University of California, Irvine, California 92717
Received November 16, 1990; Revised Manuscript Received February 22, 1991

ABSTRACT: Time-resolved absorption changes of photoexcited bacteriorhodopsin were measured with a gated multichannel analyzer between 100 ns and 100 ms at six temperatures between 5 and 30 °C. The energetics of the chromophore reaction cycle were analyzed on the basis of a model containing a single cycle and reversible reactions. The calculated thermodynamic parameters provide insights to general principles of the active transport. They indicate that in this light-driven proton pump the free energy is retained after absorption of the photon as the enthalpy of the pK_a shift in the chromophore which allows deprotonation of the Schiff base. Part of the excess free energy is dissipated at the "switch" step where the reaction and transport cycles are coupled, and the rest at the chromophore recovery step. All other reactions take place near equilibrium. The "switch" step is the $M_1 \rightarrow M_2$ transition in the reaction cycle [Váró, G., & Lanyi, J. K. (1991) *Biochemistry* (preceding paper in this issue)]. It provides for return of the chromophore pK_a to its initial value so the Schiff base will become a proton acceptor, for reordering access of the Schiff base from one side of the membrane to the other, and for unidirectionality of the proton transfer. Conformational energy of the protein, acquired during the "switch" step, drives the completion of the photocycle.

The light-driven proton pump of halobacteria, bacteriorhodopsin (BR),[1] is the simplest known active membrane transport system. The desire to understand this protein and thereby gain general insights to ion pumps has motivated two decades of intense research. The general features of the transport mechanism in this system are now understood. Recent studies from several laboratories on the consequences of site-specific and natural mutations, advances in vibrational spectroscopy, and a recent high-resolution structural model (Henderson et al., 1990) have provided much missing information, and suggest the following sequence (cf. Figure 1 for an approximate representation of the geometry near the retinal): Adsorption of a photon by the *all-trans*-retinal-containing chromophore produces an excited state which decays first into a distorted (Braiman et al., 1982; Smith et al., 1984) and then into a relaxed (Aton et al., 1977) 13-cis isomeric state. This is followed by transfer of the Schiff base proton to D85 (Braiman et al., 1988; Butt et al., 1989; Tittor et al., 1989) and then to the external side of the cell membrane. The Schiff base is then reprotonated from D96 (Butt et al., 1989; Tittor et al., 1989; Gerwert et al., 1989, 1990a; Otto et al., 1989) which in turn gains a proton from the cytoplasmic side. The retinal returns to the all-trans configuration and thereby completes the cycle. In this report, we examine the thermodynamics of these reactions and what they imply for the mechanism. This provides a broad perspective on energy coupling which may be useful for understanding the principles of active transport in general.

The retinal chromophore of BR absorbs intensely in the visible (Lozier et al., 1975) and has vibrational modes with largely identified frequencies (Smith et al., 1985). The intermediates of the reaction cycle were described by Lozier et al. (1975) and others; they were labeled as J, K, L, M, N, and O. The most blue-shifted state, M, containing a deprotonated Schiff base, is the key intermediate. After much study and numerous proposed models, the stubborn kinetic complexities of the rise and decay of M (and of some of the other intermediates) have been described satisfactorily by means of a single-cycle reaction sequence containing reverse reactions with significant rates (Otto et al., 1989; Váró & Lanyi, 1990a–c, 1991; Ames & Mathies, 1990; Gerwert et al., 1990a). Nagle et al. (1982) had already discussed the problems with models containing only irreversible reactions. Likewise, our recent results make complex models containing parallel reaction pathways and only irreversible reactions seem unlikely (Váró & Lanyi, 1990a,b, 1991). The time resolution available in our studies has allowed measurement of the kinetics of all species after K. Reverse reactions have been detected between K and L, L and M, M and N, and N and O. Two features of this model are not as yet generally agreed upon, but are suggested by our data and those of another group (Váró & Lanyi, 1990a–c, 1991; Gerwert et al., 1990a). First, there appear to be two similar M states connected by an irreversible reaction because otherwise L could not approach zero concentration at times where M (i.e., M_1 *plus* M_2) is maximal. This is particularly evident in the D96N mutant protein where the M state (i.e., M_2) is stabilized and the kinetics of L can be very accurately described, and in monomeric BR where the two M states can be distinguished also spectroscopically (Váró & Lanyi, 1991). Second, branching at N seems to occur because under some conditions O and BR rise simultaneously and with similar time constants (Váró et al., 1990). The data in this report are interpreted in terms of a model containing these features.

Materials and Methods

Growth of *Halobacterium halobium* strain S9 and preparation of purple membranes containing BR were described previously (Oesterhelt & Stoeckenius, 1974). Likewise, the instrumentation to measure time-resolved difference spectra

† These results were presented in part at the IVth International Conference on Retinal Proteins, Santa Cruz, CA, July 22–28, 1990. This work was supported by a grant from the National Institutes of Health (GM 29498).
‡ Permanent address: Biological Research Center of the Hungarian Academy of Sciences, Szeged, Hungary.

[1] Abbreviations: BR, bacteriorhodopsin; J, K, L, M_1, M_2, N, and O, intermediates of the bacteriorhodopsin photocycle; D96N, bacteriorhodopsin in which aspartate-96 is replaced with asparagine.

0006-2960/91/0430-5016$02.50/0

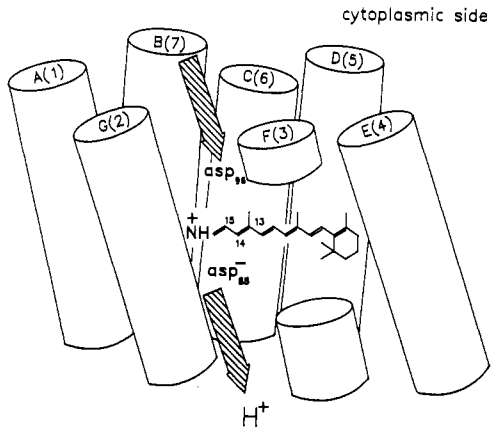

FIGURE 1: Approximate structure of bacteriorhodopsin, helical assignments [letters refer to predicted helices in the amino acid sequence and numbers to those in electron density maps; e.g., see Engelman et al. (1980)], and the locations of the retinal Schiff base (shown as NH^+) and important residues. Helix F(3) is partially cut away. Henderson et al. (1990) contain details of the structure. The two arrows indicate proton release from the Schiff base via D85 and the protonation of D96 after it reprotonated the Schiff base. Unresolved questions discussed in this report include the unidirectionality of the proton transfer and thermodynamic evidence for protein conformational changes in coupling the reactions of the chromophore to transport.

and treatment of the data were as before (Zimányi et al., 1989; Váró & Lanyi, 1990b).

Results

Deriving the Kinetics of the Photocycle from Time-Resolved Difference Spectra. Traditionally, interconversions of photocycle intermediates have been followed by measuring the time dependence of adsorption changes at a few selected wavelengths. With optical multichannel spectroscopy (Zimányi et al., 1989), it has been possible to obtain high-resolution difference spectra which contain the absorptions of all transient species present at a given time after photoexcitation *minus* the spectrum of the depleted BR. Figure 2 shows measured difference spectra in 100 mM NaCl, pH 7.0, at delay times between 100 ns and 100 ms after photoexcitation at 5 and 30 °C. Spectra at 20 °C under the same conditions are given elsewhere (Váró & Lanyi, 1991). Evaluating a kinetic model requires decomposing such difference spectra into spectra of the intermediates and calculating their time-dependent concentrations. The difference spectra do not contain enough information, however, to define both component spectra and kinetics. In our approach [described in detail in Váró and Lanyi (1990b)], this inherent problem was overcome by requiring the calculated absorption spectra to obey reasonable criteria. First, the spectra cannot contain negative absorptions. Second, from known rhodopsin spectra and the properties of retinal excited states, one expects single peaks and half-widths within certain limits. When the spectra of the five intermediates were required to obey these criteria simultaneously, the positions of the absorption maxima became fixed to within a few nanometers, and the range of possible amplitudes was narrowed to give virtually a single set of spectra. The absorption spectra for K, L, M, N, and O in Figure 2A of the preceding paper (Váró & Lanyi, 1991) are the result of such a decomposition. Error analysis indicated that changes of ±10% in the amplitudes did not seriously affect the model and the derived thermodynamic parameters (cf. below). We are confident that the accuracy of the calculated spectra is within these limits. They are essentially identical with spectra calculated from BR films (Váró & Lanyi, 1990b), and their amplitudes are very close to those determined in earlier time-resolved and low-temperature measurements (Lozier et al., 1975; Becher et al., 1978; Zimányi et al., 1989). An independent basis for judging them is provided by the linear relationship of the visible absorption maxima of retinal chromophores to their ethylenic stretch frequency (Aton et al., 1977); the positions of the maxima agree well with those predicted.

Once the spectra of the intermediates were determined from the data at 20 °C, they provided a set of component difference

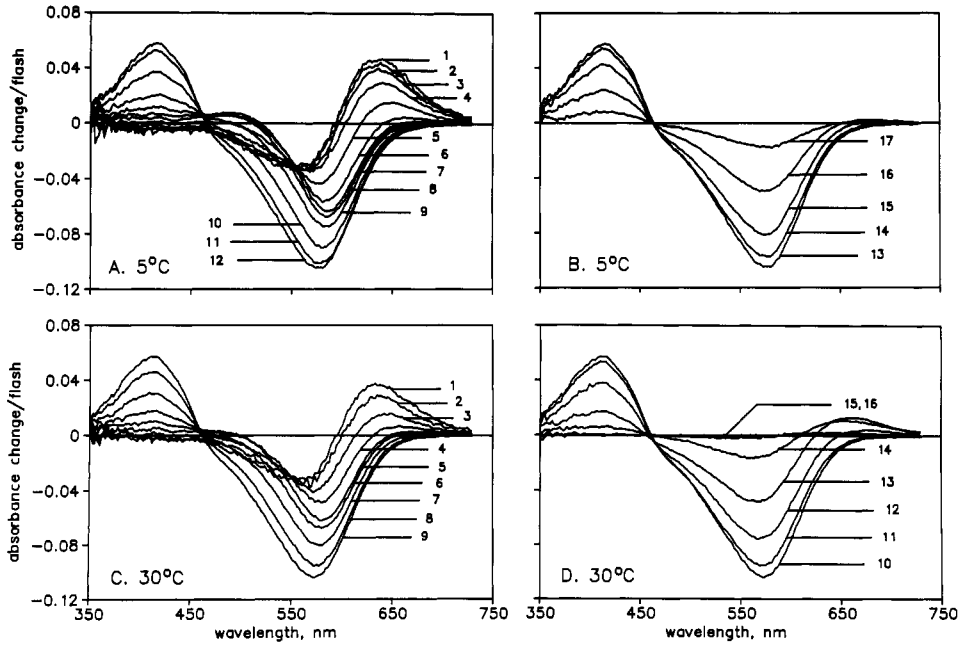

FIGURE 2: Time-resolved difference spectra of photoexcited bacteriorhodopsin at 5 and 30 °C. The spectra were determined after subnanosecond laser pulses (580 nm) with a gated optical multichannel analyzer, as described before (Zimányi et al., 1989). Delay times between the flash and the measurements are indicated by numbers from 1 through 17 which refer to 100 ns, 250 ns, 600 ns, 1.5 μs, 4 μs, 10 μs, 25 μs, 60 μs, 150 μs, 400 μs, 1 ms, 2.5 ms, 6 ms, 15 ms, 40 ms, and 100 ms. Conditions: BR (purple membrane suspensions) at 40 nmol/mL, in 100 mM NaCl/50 mM phosphate, pH 7.0, at the indicated temperatures.

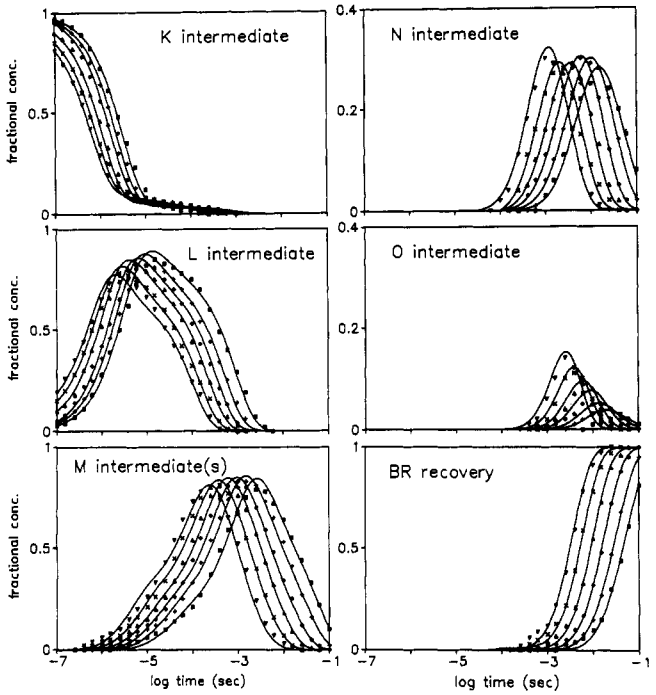

FIGURE 3: Time-dependent fractional concentrations of K, L, M (M_1 *plus* M_2), N, O, and BR at six temperatures. Symbols: (■) 5 °C; (+) 10 °C; (◇) 15 °C; (△) 20 °C; (×) 25 °C; (▽) 30 °C. Lines are the best fits to the model in Figure 4.

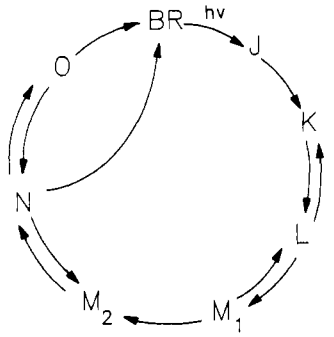

FIGURE 4: Suggested reaction scheme for the photocycle of *all-trans*-bacteriorhodopsin. Evidence for various parts of this model has been given in earlier reports (Otto et al., 1989; Vârô & Lanyi, 1990a–c, 1991; Vârô et al., 1990; Ames et al., 1990; Gerwert et al., 1990b). The intermediate K can be resolved into an early and a late K state, K and KL (Shichida et al., 1983), but at 100 ns or later, only the second species is observable.

spectra whose appropriately weighted sums reproduced the measured difference spectra at all temperatures and yielded the fractional concentrations of the intermediates at each delay time. Figure 3 shows the results of such calculations for the intermediates K, L, M (i.e., M_1 *plus* M_2), N, and O, and the recovery of bacteriorhodopsin at six temperatures, as well as the best fits of numerical solutions of the model in Figure 4. The fits (lines) in Figure 3 define the rate constants of all interconversions after K in the model.

Activation Energies in the Bacteriorhodopsin Reaction Cycle. The temperature dependencies of the rate constants which produced the fits in Figure 3 permit evaluation of the thermodynamic parameters of the reactions. Equations 1 and 2 relate the enthalpies, entropies, and free energies of activation

$$\ln k_i = \ln \frac{kT}{\hbar} + \frac{\Delta S_i^*}{R} - \frac{\Delta H_i^*}{RT} \quad (1)$$

$$\Delta G_i^* = \Delta H_i^* - T\Delta S_i^* \quad (2)$$

to the rate constants and the temperature where k_i is the rate

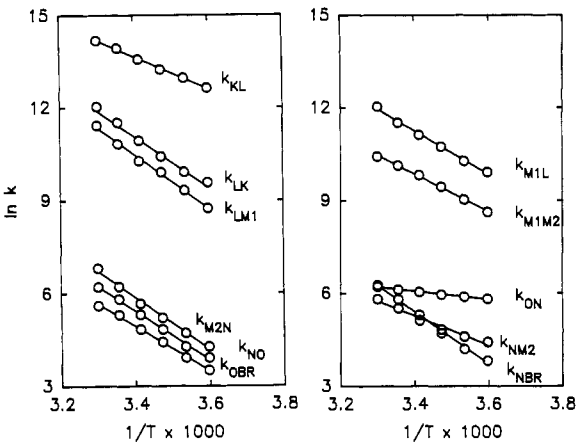

FIGURE 5: Eyring plots of the rate constants of the photocycle reactions. The rate constants are from Figure 3; the lines are nonlinear least-squares regressions based on eq 1. Average of standard errors is ±2 kJ/mol for ΔH^* and ±6 J/(mol·K) for ΔS^*.

constant of the ith reaction, k is the Boltzmann constant, T is the absolute temperature, $\hbar$ is Planck's constant, R is the gas constant, and ΔG_i^*, ΔH_i^*, and ΔS_i^* are the free energy, enthalpy, and entropy of activation of the ith reaction, respectively. ΔH and ΔS are both functions also of the heat capacity change, ΔC_p, if any, between the initial and final states: $\delta\Delta H = \Delta C_p \delta T$ and $\delta\Delta S = \Delta C_p \delta T/T$. For protein folding reactions, plots of log k vs $1/T$ will be curved because the heat capacity change of the accompanying reorganization of surface water is anomalously large and ΔH and ΔS thereby become temperature dependent (Sturtevant, 1977; Baldwin, 1986; Murphy et al., 1990). Figure 5 shows the data and nonlinear regressions between 5 and 30 °C. The uniform standard deviations throughout indicated that any errors of the fitting in Figure 3 were distributed evenly over all rate constants and temperatures. The good linearity suggests that in this system ΔH^* and ΔS^* are not temperature dependent; this will be assumed in the calculations. The assumption seems reasonable also because the amount of surface water is unlikely to change during reactions in the interior of this membrane protein. We calculate that the equivalent of the loss or gain of surface water around a single phenylalanine residue in the protein, i.e., a ΔC_p of about 300 J/mol·K), would have caused noticable nonlinearity in Figure 5.

Figures 6A,B and 7 show the enthalpies, entropies, and free energies of activation. The ΔH^* and ΔS^* values are temperature-independent; the ΔG^* values are calculated for 20 °C. The enthalpy, entropy, and free energy differences between intermediates are of greater immediate interest, however. The ΔH, ΔS, and ΔG values between K and L, L and M_1, M_2 and N, and N and O are defined by the data in Figure 5 because for these intermediates the heights of the activation barriers are given from both directions. Because the $M_2 \rightarrow M_1$, BR → N, and BR → O back-reactions could not be measured, the heights of the K–L–M_1 and M_2–N–O segments relative to BR were not defined by the data. These were calculated by using data from earlier reports. The calorimetric enthalpy gain after absorption of a photon (Birge & Cooper, 1983) and the enthalpy loss at M relative to BR (Ort & Parson, 1979; Garty et al., 1982) have been measured. The reported values were based on the assumptions that the quantum yield was 0.3 and the proton stoichiometry 1.7, respectively. The former is now confirmed as 0.6 (Tittor & Oesterhelt, 1990; Govindjee et al., 1990), and a stoichiometry of 1 H^+ per photocycle (Drachev et al., 1984; Grzesiek & Dencher, 1986; Vârô & Lanyi, 1990c) is accepted [but see

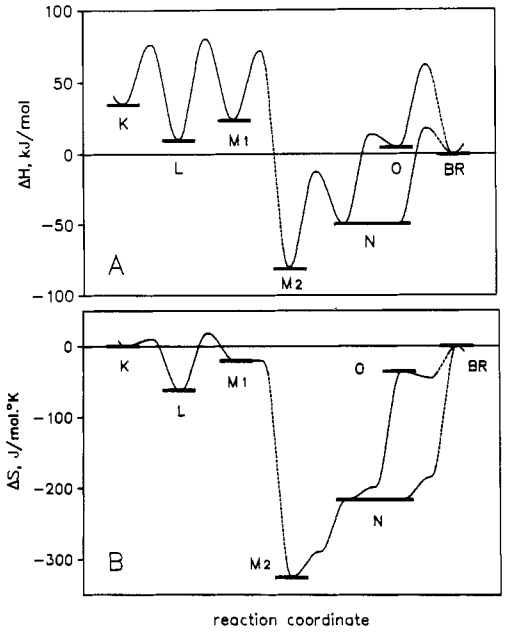

FIGURE 6: Calculated enthalpy (A) and entropy (B) changes relative to bacteriorhodopsin during the photocycle. Dotted lines indicate magnitudes based on earlier calorimetric data or assumptions, as explained in the text.

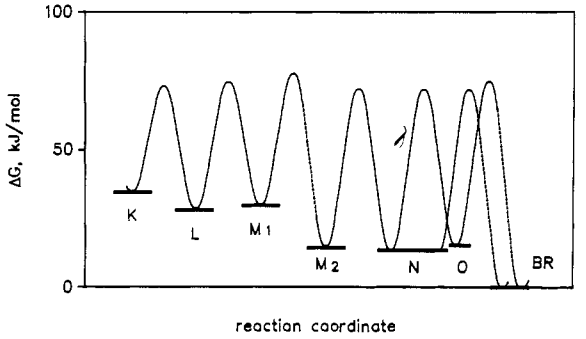

FIGURE 7: Calculated free energy changes at 20 °C relative to bacteriorhodopsin during the photocycle. Dotted lines indicate magnitudes based on earlier calorimetric data or assumptions, as explained in the text.

Birge et al. (1989) for another opinion]. We recalculated the reported values accordingly (ΔH between BR and K is 35 kJ/mol; between M_2 and BR, −80 kJ/mol) and assumed further that ΔS is negligible before K (cf. below). The 30 kJ/mol free energy after L (Figure 7) was apportioned as shown because transporting a proton against 180 mV requires at least 17 kJ/mol which is balanced mainly by the $M_1 \rightarrow M_2$ step, and we have found that the free energy decrease here is at least 13 kJ/mol (Váró & Lanyi, 1991). On the other hand, a thermal O → BR equilibrium favors BR by more than 100-fold, which would be equivalent to a free energy difference of 11.4 kJ/mol between O and BR. Transitions calculated with these considerations are shown with dotted lines.

Discussion

The free energy acquired in the J state drives all thermal interconversions of the chromophore and the protein, as well as the proton-transfer reactions. It is evident from the data (Figure 7) that most of the excess free energy of K is lost at the $M_1 \rightarrow M_2$ reaction and during the recovery of BR, rather than continuously throughout the sequence. The intervening interconversions proceed with little change in ΔG. This is similar to other active transport systems in which binding energy differences for ATP and its hydrolysis products drive the reaction and translocation cycles. Thus, the energetics of the BR photocycle can be discussed in terms of the coupling principles postulated earlier for other active transport systems (Tanford, 1983), with only minor changes:

(1) Coupling between the Driving Reaction and the Transport Requires Two Conformational States. Efficient coupling requires that thermal relaxation of the chromophore should not occur without vectorial proton transfer and that proton transfer should not occur without the corresponding transformation of the chromophore. The place where the transport cycle limits the reaction cycle, and vice versa, is the coupling step. The vectorial proton transfer implies *two conformational states which allow access of the proton to one or the other membrane side but not to both at the same time.* Although movements of the protein backbone have been detected [e.g., see Engelhard et al. (1985), Braiman et al. (1987), Dencher et al. (1989), and Gerwert et al. (1990b)], this duality, also referred to as the "switch", must originate in or near the Schiff base of the chromophore. As have others (Nagle & Mille, 1981; Schulten et al., 1984), we suggest that it is the molecular rationale for the two M species (Figure 4), M_1 being in equilibrium with L and connected to the release of a proton on the external side, and M_2 being in equilibrium with N and connected to the uptake of a proton on the cytoplasmic side. The switch is thereby placed just before the proton passes from D96 through the principal hydrophobic barrier (Henderson et al., 1990) to the Schiff base. This motif is inherent in the kinetic model (Figure 4) and suggested by the high-resolution structural model for the protein also (Henderson et al., 1990).

The molecular nature of the switch is the outstanding question in the photocycle. It is *not* linked to the reisomerization around the 13–14 carbon bond of the retinal, which takes place two steps later. In the first of two proposed alternatives, it is nonetheless the retinal which plays the key role: absorption of the photon causes isomerization around both 13–14 and 14–15 carbon bonds, producing 13-*cis*,14-*s*-*cis*-retinal (Gerwert & Siebert, 1986). Deprotonation of the Schiff base would decrease the barrier for rotation around single bonds, but raise it for double bonds (Tavan et al., 1985), allowing relaxation to the 13-cis,14-s-trans configuration during the M state. This would reorient the Schiff base and alter its access from D85 toward the strategic proton donor residue D96. However, the spectroscopic evidence for such isomerization has been disputed (Fodor et al., 1988a), and as an alternative, a protein conformational change (the "C-T model") was proposed instead (Fodor et al., 1988b). Data of various kinds have indeed revealed conformational differences between the BR and M states (Engelhard et al., 1985; Braiman et al., 1987; Dencher et al., 1989; Gerwert et al., 1990b).

(2) At the Coupling Reaction, Free Energy Is Transferred from the Active Site to the Protein. The results in this study are consistent with enthalpy changes measured earlier (Ort & Parson, 1979; Garty et al., 1982) directly by photoacoustic spectroscopy. These groups found, unexpectedly at that time, that after proton release enthalpy decreased, by about 80 kJ/mol, to below that of the initial BR state. The enthalpy increase which followed occurred during the recovery of the chromophore. The reaction associated with the former is now identified as $M_1 \rightarrow M_2$, while those with the latter as the M_2 to N, N to O, and N to BR transitions. Figure 6A indicates that the M_2 to BR recovery pathways result in a total enthalpy rise of about 80 kJ/mol or about the same as the decrease calculated from the results of Ort and Parson (1979). As suggested by these authors, these endothermic reactions must be driven by negative entropy acquired by the system; at 20

°C, about −300 J/(mol·K) is required. Since the reactions before M_1 produce a negligible net entropy decrease (Figure 6B), this would have to be obtained either before K or during the $M_1 \rightarrow M_2$ reaction. Large entropy changes in this system must originate from conformational changes of the protein or the lipid because the chromophore (which includes the retinal and the residues with which it directly interacts) does not contain sufficient degrees of internal freedom. Data for a large number of protein unfolding reactions (Sturtevant, 1977; Baldwin, 1986; Murphy et al., 1990) indicate that −300 J/(mol·K) would be obtained upon the folding of 15–20 residues (provided that a decrease of bound water is not considered). In view of the rapidity (10^9 s^{-1} and faster) of the reactions preceding K, protein motions of this magnitude before K seem unlikely. On the other hand, the rate constant of the $M_1 \rightarrow M_2$ reaction (2×10^4 s^{-1} at 20 °C) is just at the upper limit for large conformational transitions in proteins, and the large enthalpy decrease here (Figure 6A) would supply the required free energy. It seems that this is the only step in which the large negative entropy could have been acquired.

Thus, it appears that before the coupling reaction excess free energy is confined mostly to the chromophore, but afterward it will have been transferred to the protein. A conformational change at the $M_1 \rightarrow M_2$ reaction is consistent with the observation that even modest removal of water causes its drastic slowing (Vārō & Lanyi, 1990b). From M_2 to N, entropy rises by about 100 J/(mol·K) (Figure 6B). N returns to BR via O over two barriers, or directly over a single barrier. Almost all of the rest of the entropy rise, about 200 J/(mol·K), is realized between N and O. Thus, the conformational change which returns the protein to its initial state is completed as N decays, consistently with the scheme in Figure 4 in which O is not an obligatory part of the reaction sequence.

(3) The Free Energy Changes of Most of the Interconversions Should Be Close to Zero. This general rule of enzyme catalysis proposed by Albery and Knowles (1976) for fully reversible systems is applicable to most of the steps in pumps also. Small free energy changes will prevent accumulation of intermediate species and the ensuing restrictions on reaction rates. The principle is realized effectively in the BR photocycle where the free energy levels of K, L, and M_1 and of M_2, N, and O are very close together (Figure 7). This is true also for some of the reactions in the photocycle of halorhodopsin (Spencer & Dewey, 1990), a related retinal-based chloride ion transport system. Likewise, compensation of ΔH by $T\Delta S$ was observed for most of the steps in the erythrocyte glucose and leucine carriers (Walmsley & Lowe, 1987).

(4) Irreversibility of the Transport Is Ensured by a Step (or Steps) with a Large Free Energy Decrease. Since all free energy gained in the J state is lost when bacteriorhodopsin recovers, it follows from rule 3 that there must be at least one step in the reaction cycle with a large decrease in free energy. It is this large free energy drop which results in unidirectionality of the pump. In BR, there are two such steps (Figure 7): $M_1 \rightarrow M_2$, and the recovery of BR at the end of the photocycle. The drops of about 15 kJ/mol ensure virtual irreversibility, i.e., the back-reactions are slower by nearly 3 orders of magnitude. Irreversibility of the late steps and equilibria strongly in favor of BR are required in order to fully recover the chromophore and make it possible to take advantage of high proton fluxes. Irreversibility of the $M_1 \rightarrow M_2$ step, on the other hand, affects the back-pressure from the proton electrochemical potential. Proton translocation ends effectively with the N intermediate (Otto et al., 1989; Kouyama & Nasuda-Kouyama, 1989). With reversibility in all steps prior to N, the proton gradient created would drive all reactions backward as far as K (or J) and thereby reverse all transport steps including proton release. The large barrier of the $M_2 \rightarrow M_1$ back-reaction (Figure 7) prevents this. Indeed, protonmotive force causes the piling up of M (i.e., M_2) (Groma et al., 1984; Helgerson et al., 1985). It is important to emphasize that the observed large drop in free energy (i.e., irreversibility) at this step is a consequence of the fact that the proton gradient was dissipated in our experiments with open purple membrane sheets. In a coupled system, the proton potential created would balance this drop in free energy.

The proton transport is based on directed changes in the pK_as of the Schiff base and specific groups in the protein (Stoeckenius et al., 1979; Fischer & Oesterhelt, 1979): In the $L \rightarrow M_1$ reaction, the Schiff base is a proton donor, but in the $M_2 \rightarrow N$ reaction, it is an acceptor. The relative proton affinities will determine the free energy changes during the protonation reactions. Because the ΔG values of proton transfer to and from the Schiff base are close to zero (Figure 7), the pK_as of the proton donors and acceptors during these events will have been essentially the same. Estimates for the pK_as of the Schiff base and D85 before photoexcitation are available; they are above 10 (Druckmann et al., 1982) and 2–3 [Rothschild et al., 1981; Braiman et al., 1988; and as discussed by Subramaniam et al. (1990)], respectively. The pK_a of D96 has been estimated to be 10.5 (Otto et al., 1989). Clearly, the proton affinities are changed during the photocycle as the pK_as of the Schiff base and D85 approach one another at the $L \rightarrow M_1$ step. In halorhodopsin, a related system, protonation equilibria with a variety of added bases with different pK_as had indicated that the Schiff base pK_a was lowered to 4.3 during the photocycle (Lanyi, 1986). A free energy increase of 35 kJ/mol in K (Figure 7) would produce somewhat over 6 units of pK_a change; that this is less than what appears to be required[2] may reflect either underestimation of the ΔG of K or overestimation of the needed pK_a changes because of interactions of charged residues with the Schiff base. In any case, it is likely that in the L species all, or nearly all, of the acquired free energy will be manifested in the changed pK_a(s) of the group(s) which participate(s) in the proton transfer.

For D96 to be an effective donor in the reprotonation of the Schiff base, independent of external pH up to above 9 as observed (Otto et al., 1989; Vārō & Lanyi, 1990a), its pK_a during the $M_2 \rightarrow N$ step cannot be lower than the pH in the medium. Thus, to allow its reprotonation, the pK_a of the Schiff base must be raised again, to above 9, at this point in the photocycle. A return of the pK_a of the Schiff base to its original high value is as expected if, as described above, part of the excess free energy is used to raise the proton potential while the rest is transferred from the chromophore to the protein at this step. It also follows from this scheme that the reason for conserving some of the free energy in the protein is that completion of the photocycle could not take place without a second loss of ΔG. We conclude that *the $M_1 \rightarrow M_2$ reaction fulfills three essential roles in the transport: (1) it causes the Schiff base to change from proton donor to acceptor; (2) it changes access of the Schiff base to protons from one side of the membrane to the other; and (3) it ensures coupling to the proton gradient and unidirectionality of the reaction cycle.*

The reaction mechanism and the thermodynamic principles which underlie the proton transport are thus beginning to be

[2] A recent recalculation of the excess enthalpy content of K gave about 45 kJ/mol, a higher value than used in Figure 6A (R. Birge, personal communication).

understood, but many important details are missing. D212, Y185, Y57, and probably R82 are located in a position to interact, individually or in a concerted way, with the Schiff base (Henderson et al., 1990), and their participation in proton transfer is likely (Braiman et al., 1988; Gerwert et al., 1989, 1990a) but not yet defined. The means of proton conduction between D96 and the Schiff base are not known. Most importantly, the coupling step between retinal chromophore and transport needs to be explained in molecular terms.

ACKNOWLEDGMENTS

We are indebted to S. H. White, R. Jacobs, S. Fraser, G. Eyring, W. W. Parson, R. Henderson, and P. Mitchell for critical reading of the manuscript and suggestions.

Registry No. H^+, 12408-02-5.

REFERENCES

Albery, W. J., & Knowles, J. R. (1976) *Biochemistry 15*, 5631–5640.
Ames, J. B., Fodor, S. P. A., & Mathies, R. A. (1990) *Biochemistry 29*, 7181–7190.
Aton, B., Doukas, A. G., Callender, R. H., Becher, B., & Ebrey, T. G. (1977) *Biochemistry 16*, 2995–2999.
Baldwin, R. L. (1986) *Proc. Natl. Acad. Sci. U.S.A. 83*, 8069–8072.
Becher, B., Tokunaga, F., & Ebrey, T. G. (1978) *Biochemistry 17*, 2293–2300.
Birge, R. R., & Copper, T. M. (1983) *Biophys. J. 42*, 61–69.
Birge, R. R., Cooper, T. M., Lawrence, A. F., Masthay, M. B., Vasilikis, C., Zhang, C.-F., & Zivodetzki, R. (1989) *J. Am. Chem. Soc. 111*, 4063–4074.
Braiman, M., & Mathies, R. (1982) *Proc. Natl. Acad. Sci. U.S.A. 79*, 403–407.
Braiman, M., Ahl, P. L., & Rothschild, K. J. (1987) *Proc. Natl. Acad. Sci. U.S.A. 84*, 5221–5225.
Braiman, M. S., Mogi, T., Marti, T., Stern, L. J., & Khorana, H. G. (1988) *Biochemistry 27*, 8516–8520.
Butt, H. J., Fendler, K., Bamberg, E., Tittor, J., & Oesterhelt, D. (1989) *EMBO J. 8*, 1657–1663.
Dencher, N. A., Dresselhaus, D., Zaccai, G., & Büldt, G. (1989) *Proc. Natl. Acad. Sci. U.S.A. 86*, 7876–7879.
Drachev, L. A., Kaulen, A. D., & Skulachev, V. P. (1984) *FEBS Lett. 178*, 331–335.
Druckmann, S., Ottolenghi, M., Pande, A., Pande, J., & Callender, R. H. (1982) *Biochemistry 21*, 4953–4959.
Engelhard, M., Gerwert, K., Hess, B., Kreutz, W., & Siebert, F. (1985) *Biochemistry 24*, 400–407.
Engelman, D. M., Henderson, R., McLachlan, A. D., & Wallace, B. A. (1980) *Proc. Natl. Acad. Sci. U.S.A. 77*, 2023–2027.
Fischer, U., & Oesterhelt, D. (1979) *Biophys. J. 28*, 211–230.
Fodor, S. P., Pollard, W. T., Gebhard, K., van der Berg, E. M., Lugtenburg, J., & Mathies, R. A. (1988a) *Proc. Natl. Acad. Sci. U.S.A. 85*, 2156–2160.
Fodor, S. P., Ames, J. B., Gebhard, K., van der Berg, E. M., Stoeckenius, W., Lugtenburg, J., & Mathies, R. A. (1988b) *Biochemistry 27*, 7097–7101.
Garty, H., Caplan, S. R., & Cahen, D. (1982) *Biophys. J. 37*, 405–415.
Gerwert, K., & Siebert, F. (1986) *EMBO J. 5*, 805–811.
Gerwert, K., Hess, B., Soppa, J., & Oesterhelt, D. (1989) *Proc. Natl. Acad. Sci. U.S.A. 86*, 4943–4947.
Gerwert, K., Souvignier, G., & Hess, B. (1990a) *Proc. Natl. Acad. Sci. U.S.A. 87*, 9774–9778.
Gerwert, K., Hess, B., & Engelhard, M. (1990b) *FEBS Lett. 261*, 449–454.
Govindjee, R., Balashov, S. P., & Ebrey, T. G. (1990) *Biophys. J. 58*, 597–608.
Groma, G. I., Helgerson, S. L., Wolber, P. K., Beece, D., Dancshazy, Zs., Keszthelyi, L., & Stoeckenius, W. (1984) *Biophys. J. 45*, 985–992.
Grzesiek, S., & Dencher, N. A. (1986) *FEBS Lett. 208*, 337–342.
Helgerson, S. L., Mathew, M. K., Bivin, D. B., Wolber, P. K., Heinz, E., & Stoeckenius, W. (1985) *Biophys. J. 48*, 709–719.
Henderson, R., Baldwin, J. M., Ceska, T. A., Zemlin, F., Beckmann, E., & Downing, K. H. (1990) *J. Mol. Biol. 213*, 899–929.
Kouyama, T., & Nasuda-Kouyama, A. (1989) *Biochemistry 28*, 5963–5970.
Lanyi, J. K. (1986) *Biochemistry 25*, 6706–6711.
Lozier, R. H., Bogomolni, R. A., & Stoeckenius, W. (1975) *Biophys. J. 15*, 955–963.
Murphy, K. P., Privalov, P., & Gill, S. J. (1990) *Science 247*, 559–561.
Nagle, J. F., & Mille, M. (1981) *J. Chem. Phys. 74*, 1367–1372.
Nagle, J. F., Parodi, L. A., & Lozier, R. H. (1982) *Biophys. J. 38*, 161–174.
Oesterhelt, D., & Stoeckenius, W. (1974) *Methods Enzymol. 31*, 667–678.
Ort, D. R., & Parson, W. W. (1979) *Biophys. J. 25*, 355–364.
Otto, H., Marti, T., Holz, M., Mogi, T., Lindau, M., Khorana, H. G., & Heyn, M. P. (1989) *Proc. Natl. Acad. Sci. U.S.A. 86*, 9228–9232.
Rotschild, K. J., Zagaeski, M., & Cantore, W. A. (1981) *Biochem. Biophys. Res. Commun. 103*, 483–489.
Schulten, K., Schulten, Z., & Tavan, P. (1984) in *Information and Energy Transduction in Biological Membranes* (Bolis, A., Helmreich, H., & Passow, H., Eds.) pp 113–131, Alan R. Liss, Inc., New York.
Shichida, Y., Matuoka, S., Hidaka, Y., & Yoshizawa, T. (1983) *Biochim. Biophys. Acta 723*, 240–246.
Smith, S. O., Myers, A. B., Pardoen, J. A., Winkel, C., Mulder, P. P. J., Lugtenburg, J., & Mathies, R. A. (1984) *Proc. Natl. Acad. Sci. U.S.A. 81*, 2055–2059.
Smith, S. O., Lugtenburg, J., & Mathies, R. A. *J. Membr. Biol.* (1985) *85*, 95–109.
Spencer, D. B., & Dewey, T. G. (1990) *Biochemistry 29*, 3140–3145.
Stern, L. J., Ahl, P. L., Marti, T., Mogi, T., Duñach, M., Berkovitz, S., Rothschild, K. J., & Khorana, H. G. (1989) *Biochemistry 28*, 10035–10042.
Stoeckenius, W., Lozier, R. H., & Bogomolni, R. A. (1979) *Biochim. Biophys. Acta 505*, 215–278.
Sturtevant, J. (1977) *Proc. Natl. Acad. Sci. U.S.A. 74*, 2236–2240.
Subramaniam, S., Marti, T., & Khorana, H. G. (1990) *Proc. Natl. Acad. Sci. U.S.A. 87*, 1013–1017.
Tanford, C. (1983) *Annu. Rev. Biochem. 52*, 379–409.
Tavan, P., Schulten, K., & Oesterhelt, D. (1985) *Biophys. J. 47*, 415–430.
Tittor, J., & Oesterhelt, D. (1990) *FEBS Lett. 263*, 269–273.
Tittor, J., Soell, C., Oesterhelt, D., Butt, H.-J., & Bamberg, E. (1989) *EMBO J. 8*, 3477–3482.
Váró, G., & Lanyi, J. K. (1990a) *Biochemistry 29*, 2241–2250.
Váró, G., & Lanyi, J. K. (1990b) *Biophys. J. 59*, 313–322.
Váró, G., & Lanyi, J. K. (1990c) *Biochemistry 29*, 6858–6865.

Vârô, G., & Lanyi, J. K. (1991) *Biochemistry* (preceding paper in this issue).
Vârô, G., Duschl, A., & Lanyi, J. K. (1990) *Biochemistry 29*, 3798-3804.
Walmsley, A. R., & Lowe, A. G. (1987) *Biochim. Biophys. Acta 901*, 2229-2238.
Zimányi, L., Keszthelyi, L., & Lanyi, J. K. (1989) *Biochemistry 28*, 5165-5172.

Different Mechanisms for in Vitro Formation of Nucleosome Core Particles†

Anna M. Aragay,‡ Xavier Fernandez-Busquets, and Joan-Ramon Daban*
Departament de Bioquimica i Biologia Molecular, Facultat de Ciències, Universitat Autònoma de Barcelona, 08193-Bellaterra (Barcelona), Spain

Received October 15, 1990; Revised Manuscript Received January 14, 1991

ABSTRACT: The interaction of different histone oligomers with nucleosomes has been investigated by using nondenaturing gel electrophoresis. In the presence of 0.2 M NaCl, the addition of the pairs H2A,H2B or H3,H4 or the four core histones to nucleosome core particles produces a decrease in the intensity of the core particle band and the appearance of aggregated material at the top of the gel, indicating that all these histone oligomers are able to associate with nucleosomes. Equivalent results were obtained by using oligonucleosome core particles. Additional electrophoretic results, together with second-dimension analysis of histone composition and fluorescence and solubility studies, indicate that H2A,H2B, H3,H4, and the four core histones can migrate spontaneously from the aggregated nucleosomes containing excess histones to free core DNA. In all cases the estimated yield of histone transfer is very high. Furthermore, the results obtained from electron microscopy, solubility, and supercoiling assays demonstrate the transfer of excess histones from oligonucleosomes to free circular DNA. However, the extent of solubilization obtained in this case is lower than that observed with core DNA as histone acceptor. Our results demonstrate that nucleosome core particles can be formed in 0.2 M NaCl by the following mechanisms: (1) transfer of excess core histones from oligonucleosomes to free DNA, (2) transfer to excess H2A,H2B and H3,H4 associated separately with oligonucleosomes to free DNA, (3) transfer to excess H2A,H2B initially associated with oligonucleosomes to DNA, followed by the reaction of the resulting DNA–(H2A,H2B) complex with oligonucleosomes containing excess H3,H4, and (4) a two-step transfer reaction similar to that indicated in (3), in which excess histones H3,H4 are transferred to DNA before the reaction with oligonucleosomes containing excess H2A,H2B. The possible biological implications of these spontaneous reactions are discussed in the context of the present knowledge of the nucleosome function.

In the nucleosome, DNA interacts with the core histone octamer and forms a stable folded structure (Richmond et al., 1984). However, under appropriate solution conditions, the nucleosome core particle can undergo various conformational transitions without modification of the normal histone composition (Uberbacher et al., 1983; Yager & van Holde, 1984; Oohara & Wada, 1987b; Daban & Cantor, 1989). Moreover, the results obtained in several laboratories indicate that histones and DNA can form various complexes different from the typical nucleosome core particle. It has been found that core particle DNA can associate with different oligomers of histones H3,H4 (Simon et al., 1978; Read et al., 1985) and H2A,H2B (Oohara & Wada, 1987a; Aragay et al., 1988). It has also been found that nucleosome core particles are capable of binding more than 1 equiv of core histones in addition to the inner histone octamer (Voordouw & Eisenberg, 1978; Stein, 1979; Stein et al., 1985). The sedimentation analysis of these complexes has indicated that the additional histones are bound to the exterior of the nucleosome (Eisenberg & Felsenfeld, 1981). The histone pairs H3,H4 and H2A,H2B can also interact separately with nucleosome core particles (Eisenberg & Felsenfeld, 1981).

The altered nucleosome structures and the different DNA–histone complexes considered in the preceding paragraph could be related to the cellular function of the nucleosome. In particular, they could be involved in the mechanism of chromatin assembly. In this regard, previous physicochemical studies have demonstrated the existence of conformational transitions in the final part of the nucleosome self-assembly reaction (Daban & Cantor, 1982a,b). The involvement of DNA–(H3,H4) and DNA–(H2A,H2B) complexes in the mechanism of nucleosome self-assembly has also been investigated. It has been demonstrated that, in the presence of 0.2 M NaCl, a reaction of exchange of histone pairs allows the formation of complete nucleosome core particles from incomplete structures containing only histones H3,H4 or H2A,H2B (Aragay et al., 1988).

As in the case of DNA–(H3,H4) and DNA–(H2A,H2B) complexes, the association of histones with nucleosome core particles must also be considered in the context of the reaction of nucleosome assembly. In fact, in an early study, Stein (1979) showed that during nucleosome reassociation in 0.6 M NaCl a fraction of the core particles initially formed are complexed with an excess histone octamer, which finally is

† This work was supported in part by a grant (PB86-0029) from the Dirección General de Investigación Científica y Técnica (Spain). A.M.A. was supported by a predoctoral fellowship from the Plan de Formación de Personal Investigador (Ministerio de Educación y Ciencia, Spain) and a CIRIT grant (Generalitat de Catalunya). X.F.-B. is a recipient of a predoctoral fellowship from the Pla de Formació d'Investigadors (Generalitat de Catalunya).
* To whom correspondence should be addressed.
‡ Present address: Division of Biology, California Institute of Technology, Pasadena, CA, 91125.

0006-2960/91/0430-5022$02.50/0